Azidoblebbistatin, a photoreactive myosin inhibitor

Miklós Képiró[a], Boglárka H. Várkuti[a], Andrea Bodor[b], György Hegyi[a,c], László Drahos[d], Mihály Kovács[a,e,1], and András Málnási-Csizmadia[a,c,1]

[a]Department of Biochemistry, Institute of Biology, [b]Laboratory of Structural Chemistry and Biology, Institute of Chemistry, [c]HAS-ELTE (Eötvös Loránd University-Hungarian Academy of Sciences) Molecular Biophysics Research Group, and [e]ELTE-MTA (Eötvös Loránd University-Hungarian Academy of Sciences) "Momentum" Motor Enzymology Research Group, Eötvös Loránd University, H-1117 Budapest, Hungary; and [d]Institute of Organic Chemistry, Research Centre for Natural Sciences, Hungarian Academy of Sciences, H-1025 Budapest, Hungary

Edited by Edward D. Korn, National Heart, Lung, and Blood Institute, Bethesda, MD, and approved May 3, 2012 (received for review February 17, 2012)

Photoreactive compounds are important tools in life sciences that allow precisely timed covalent crosslinking of ligands and targets. Using a unique technique we have synthesized azidoblebbistatin, which is a derivative of blebbistatin, the most widely used myosin inhibitor. Without UV irradiation azidoblebbistatin exhibits identical inhibitory properties to those of blebbistatin. Using UV irradiation, azidoblebbistatin can be covalently crosslinked to myosin, which greatly enhances its in vitro and in vivo effectiveness. Photo-crosslinking also eliminates limitations associated with the relatively low myosin affinity and water solubility of blebbistatin. The wavelength used for photo-crosslinking is not toxic for cells and tissues, which confers a great advantage in in vivo tests. Because the crosslink results in an irreversible association of the inhibitor to myosin and the irradiation eliminates the residual activity of unbound inhibitor molecules, azidoblebbistatin has a great potential to become a highly effective tool in both structural studies of actomyosin contractility and the investigation of cellular and physiological functions of myosin II. We used azidoblebbistatin to identify previously unknown low-affinity targets of the inhibitor ($EC_{50} \geq 50$ μM) in *Dictyostelium discoideum*, while the strongest interactant was found to be myosin II (EC_{50} = 5 μM). Our results demonstrate that azidoblebbistatin, and potentially other azidated drugs, can become highly useful tools for the identification of strong- and weak-binding cellular targets and the determination of the apparent binding affinities in in vivo conditions.

interactom profile | azidation | photoactivation

Various biological processes, including muscle contraction, cell migration, differentiation, and cytokinesis require the activity of myosin II, a class of actin-based ATP-driven motor proteins. Cell-permeable small molecules that can perturb myosin functions have greatly aided the dissection and understanding of molecular processes underlying the above phenomena. Myosin II inhibitors described to date include 2,3-butanedione monoxime (BDM) (1, 2), *N*-benzyl-p-toluenesulphonamide (BTS) (3), and blebbistatin (4–6). As BDM has turned out to have a broad effect on many other proteins (7) and the inhibitory effect of BTS is limited to fast skeletal muscle myosin, until now blebbistatin has been the only potent tool for specific blocking of myosin II-dependent processes in various species and cell types. Recent data have shown that halogenated pseudilins also have nonspecific inhibitory effects on myosin II isoforms (8–10).

In vitro, blebbistatin inhibits vertebrate striated muscle and nonmuscle myosin II isoforms as well as *Dictyostelium discoideum* (*Dd*) myosin II by about 95%, with an IC_{50} of 0.5–5 μM (11). Vertebrate smooth muscle and *Acanthamoeba* myosin II are incompletely inhibited even at high blebbistatin concentrations. In vivo experiments performed with *Dd* showed that the effective inhibition of myosin II-dependent processes, including growth in suspension culture and capping of ConA receptors, require high blebbistatin concentrations (up to 100 μM) (12). The slow precipitation of blebbistatin in aqueous media resulting from its low solubility, which has not been characterized in detail, limits its applicability at high concentrations in long time-scale experiments. In addition, evidence indicates that blebbistatin may interact with partners other than myosin II (12). A crosslinkable variant of blebbistatin could therefore be effectively applied at low concentrations to eliminate cellular effects arising from low-affinity interactions. On the other hand, such a molecule could also be useful for the identification of unknown interacting proteins.

Blebbistatin blocks myosin in an actin-detached state via binding with high affinity to the myosin-ADP-P_i complex (5). This feature confers a crucial advantage in cellular studies exploring myosin function, because it prevents artifacts arising from the formation of strongly bound actomyosin complexes. Furthermore, we recently showed that myosin populates a previously inaccessible conformational state when bound to ADP and blebbistatin. This conformational state, characterized by a primed lever and high actin affinity, resembles the start point of the powerstroke (13).

Here we report the synthesis and functional characterization of (-)-para-azidoblebbistatin (referred to as azidoblebbistatin), an aryl azido derivative of blebbistatin. Aryl azides are the most popular photoaffinity agents used in many biochemical applications, such as target identification, receptor characterization, and enzymatic studies (14). By means of the aryl azide group it is possible to achieve a precisely timed covalent crosslink between the azidated ligand and its target.

Our results demonstrate that, without UV irradiation, azidoblebbistatin exhibits identical inhibitory properties to those of blebbistatin in terms of in vitro inhibition of myosin II ATPase activity and in vivo inhibition of *Dd* growth in suspension culture. The covalent crosslink between myosin and azidoblebbistatin initiated by UV irradiation has been performed successfully. The ATPase activity of the covalent complex is blocked and, in cellular experiments, crosslinked azidoblebbistatin showed an enhanced effect compared with that of high concentrations of blebbistatin. We also demonstrate that azidoblebbistatin is suitable for the identification of blebbistatin-interacting proteins in cellular extracts. The results indicate that azidoblebbistatin has a great potential to become a useful tool in the investigation of both the structural mechanism of force generation and the cellular functions of myosin II.

Results

Synthesis and Structural Characterization of Azidoblebbistatin. Synthetic strategies for the preparation of azidated compounds generally require nitro- or primary amine-derivatives as precursors (15). If these precursors are not available the synthesis could be highly difficult. The required precursors could be synthesized by direct aromatic nitration (16), but this reaction usually has low yield and results in degradation of the parent molecule or

Author contributions: M. Képiró, B.H.V., G.H., M. Kovács, and A.M.-C. designed research; M. Képiró, B.H.V., and A.M.-C. performed research; A.B. and L.D. contributed new reagents/analytic tools; M. Képiró, B.H.V., G.H., M. Kovács, and A.M.-C. analyzed data; and M. Képiró, B.H.V., M. Kovács, and A.M.-C. wrote the paper.

The authors declare no conflict of interest.

This article is a PNAS Direct Submission.

[1]To whom correspondence may be addressed. E-mail: kovacsm@elte.hu or malna@elte.hu.

This article contains supporting information online at www.pnas.org/lookup/suppl/doi:10.1073/pnas.1202786109/-/DCSupplemental.

a variety of byproducts. We found that these methods led to decomposition of blebbistatin, which rendered them inapplicable. To overcome these problems we developed a strategy based on the aromatic iodination of blebbistatin followed by a halogen azide exchange step (17–22). Iodination of blebbistatin was performed using *N*-iodosuccinimide and was catalyzed by the super acid boron trifluoride dihydrate, which was also the main solvent of the reaction (Fig. 1). To improve the acid solubility of blebbistatin, methanol was added as cosolvent. Analytical HPLC showed the formation of two products, of which the main peak was identified as (-)-para-iodo-blebbistatin by HPLC shift analysis and this intermediate led to the correct product, (-)-para-azido-blebbistatin determined by MS and NMR analysis (see below). Unsuccessful halogenation of blebbistatin was reported previously (23) using similar conditions, except for the super acid catalyst. Following purification, the halogen azide exchange reaction was achieved using sodium azide, copper (I) iodide catalyst, diamine ligand, and sodium ascorbate.

The above reaction yielded a single product that was structurally analyzed by MS (exact mass measurement) and NMR to identify the position of the azido group (see details in *SI Text*). NMR chemical shift values and coupling patterns are indicative of the substitution position. The assignment of protons, carbons, and nitrogens was performed by ^{1}H-^{1}H COSY, HSQC (Heteronuclear Single Quantum Coherence), and HMBC (Heteronuclear Multiple Bond Correlation) experiments. Based on the coupling scheme of the ^{1}H spectrum, the two doublets of the phenyl ring assigned to H2′ and H3′ with integrated intensities of two protons proved that the azido group was oriented in 4′ position on the 1-phenyl group (Fig. 1). Moreover, based on ^{1}H-^{15}N long-range correlations, we found that the H3′ doublet correlated with the N_a nitrogen of the azido group, showing the characteristic chemical shift of 90.4 ppm (see *SI Text*). Thus, the synthesis product was identified as 4H-pyrrolo[2,3-b]quinolin-4-one,1,2,3,3a-tetrahydro-3a-hydroxy-6-methyl-1(4′azido)-phenyl-, (3aS) or, briefly, (-)-para-azido-blebbistatin.

Spectral Properties and Photoreactivity of Azidoblebbistatin. We expected azidoblebbistatin to be photoreactive similarly to other arylazido compounds. Nonirradiated azidoblebbistatin showed multiple absorption peaks (Fig. 2*A*). Therefore, we investigated the spectral and structural changes occurring upon irradiation at wavelengths representing the characteristic absorption components. Upon irradiation at 310 nm, the absorption spectrum of azidoblebbistatin changed markedly (Fig. 2*A*). This behavior is indicative of photoinduced changes in molecular structure, which we investigated by analytical HPLC and MS. Successive exposures of azidoblebbistatin to 310-nm irradiation resulted in the gradual disappearance of the azidoblebbistatin peak in HPLC elution profiles, with the parallel appearance of multiple new peaks at shorter elution times (Fig. 2*B*) This behavior was expected based on earlier observations that photoreactions of aryl azido compounds result in multiple products in aqueous buffer (24). Fig. 2*C* shows the dependence of the peak integral of azidoblebbistatin on the time of irradiation at different wavelengths. Of the applied wavelengths, irradiation at 278 and 310 nm resulted in the most rapid photoreaction. In parallel with changes in the HPLC elution profile, we detected changes in MS spectra upon irradiation, confirming the occurrence of the photoreaction.

We performed control experiments with blebbistatin in which we detected no change in absorption and MS spectra (Fig. 2*A*). In earlier studies, irradiation at 365 and 450–490 nm caused changes in the absorption spectrum of blebbistatin and induced cellular toxicity (25), whereas 488-nm irradiation abolished its inhibitory properties (26). Nevertheless, our results show that the photoreactivity induced by 310-nm light is specific to azidoblebbistatin, but blebbistatin does not show any detectable change in these conditions.

Inhibition of Myosin ATPase Activity by Azidoblebbistatin Before and After Photo-Crosslinking. We determined the inhibitory properties of nonirradiated blebbistatin and azidoblebbistatin by comparing their effect on the steady state ATPase activity of *Dd* myosin II motor domain (*DdMd*). Fig. 3*A* shows that the half-maximal inhibition of the ATPase activity occurred at very similar blebbistatin and azidoblebbistatin concentrations (IC_{50} = 6.4 ± 0.9 μM and 5.2 ± 0.3 μM, respectively). Importantly, irradiation of azidoblebbistatin at 310 nm before adding it to the protein completely abolished its inhibitory effect, whereas the same treatment did not affect blebbistatin inhibition (Fig. 3*A*).

A serious limitation associated with the use of blebbistatin is its low solubility in aqueous buffers, which we determined to be even lower than it was previously reported (4). We found that the solubility of blebbistatin in the applied assay buffer at 25 °C was 7.4 ± 0.6 μM at 0.1% DMSO, and it increased quasilinearly with DMSO concentration to 80 μM at 10% DMSO (Fig. S1). The solubility of azidoblebbistatin was very similar to that of blebbistatin.

One of the important potential advantages of a covalently attached inhibitor is the elimination of limitations associated with solubility. To obtain a covalently crosslinked enzyme-inhibitor complex, 8 μM *DdMd* was treated with 10 μM azidoblebbistatin followed by UV irradiation, and azidoblebbistatin addition–UV irradiation cycles were repeated several times. The results of Fig. 3 *B* and *C* indicated that, using this procedure, practically all myosin molecules were crosslinked to the inhibitor. We verified the existence of the covalent enzyme–inhibitor complex and separated it from unbound photodegraded azidoblebbistatin by using His-tag affinity chromatography. The photoreacted azidoblebbistatin coeluted with His-tagged *DdMd* as

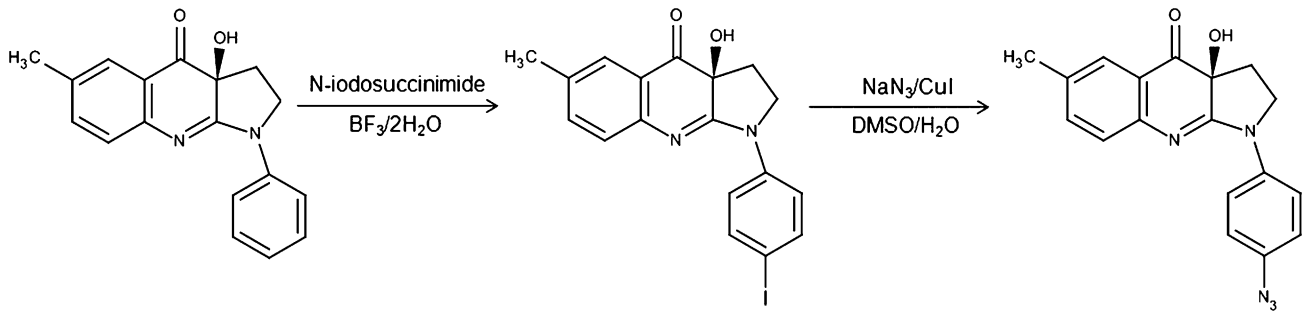

Fig. 1. Synthesis of azidoblebbistatin. Azidoblebbistatin was synthesized in a two-step reaction. Blebbistatin was treated with *N*-iodosuccinimide in the presence of boron trifuoride dihydrate. After purification the iodinated product was converted into the azide by using sodium azide and copper (I) iodide catalyst.

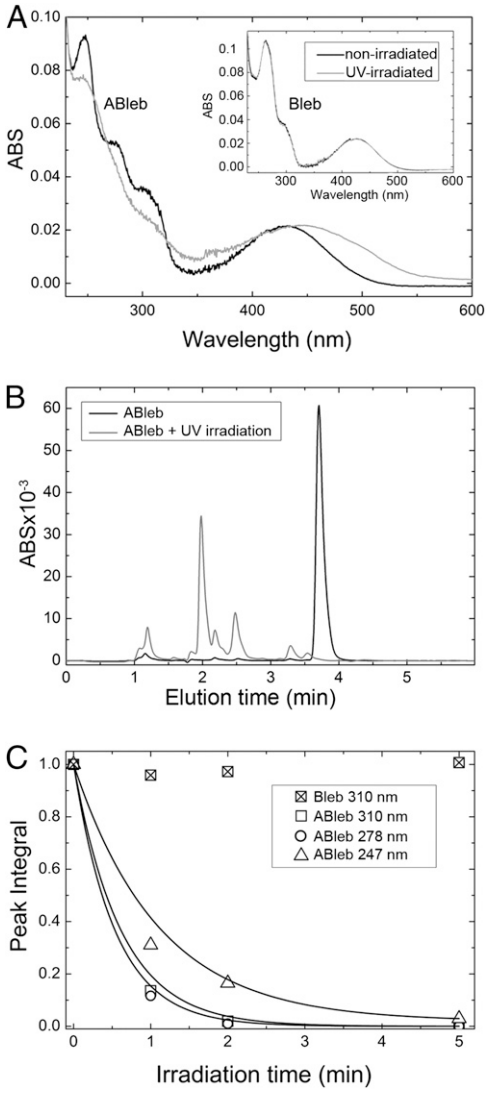

Fig. 2. Spectral properties and photoreactivity of azidoblebbistatin. (*A*) The UV-VIS spectrum of azidoblebbistatin (ABleb) was recorded before and after 310-nm UV irradiation. The spectrum went through significant changes upon irradiation, indicating successful aryl azide activation. Using the same conditions the spectrum of blebbistatin (Bleb) did not change (*Inset* shows identical nonirradiated and irradiated spectra). (*B*) Successive cycles of irradiation of azidoblebbistatin by UV light caused the disappearance of the azidoblebbistatin peak in HPLC elution profiles, with the parallel appearance of novel peaks at shorter elution times. (*C*) Gradual disappearance of the HPLC peak of azidoblebbistatin upon treatment by 310, 278, and 247 nm UV light in the absence of protein, reporting degradation of azidoblebbistatin. Under the same conditions blebbistatin degradation did not occur.

a yellow-colored fraction, providing evidence of a covalent crosslink between the molecules.

Inhibition of Cell Growth in Suspension Culture. We monitored the in vivo inhibitory effect of azidoblebbistatin and blebbistatin by following the myosin II-dependent growth of *Dd* cells in suspension culture. *Dd* ORF$^+$ cells were treated with 5 μM azidoblebbistatin or 5 μM blebbistatin, and cell growth was followed for 3 d, with or without UV irradiation occurring every 24 h. A large fraction of azidoblebbistatin-treated cells became multinuclear, similarly to blebbistatin-treated ones, because of the lack of the contraction of the cleavage furrow during cytokinesis

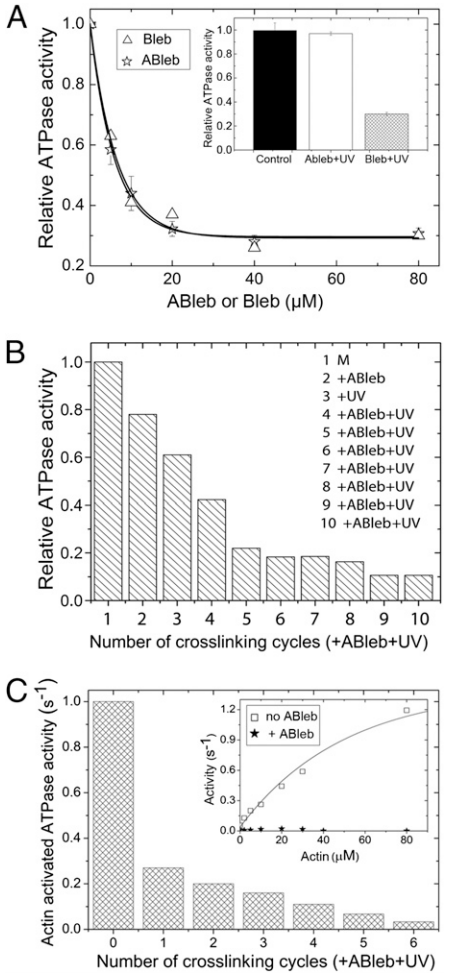

Fig. 3. Myosin ATPase inhibition by azidoblebbistatin in the absence and presence of actin. (*A*) Inhibition of the basal (actin-free) ATPase activity of *DdMd* in the absence of irradiation. Relative ATPase activities of 2 μM *DdMd* at increasing concentrations of blebbistatin (Bleb) or azidoblebbistatin (ABleb) are shown. Hyperbolic fits to the datasets yielded IC_{50} values of 6.4 ± 0.9 μM and 5.2 ± 0.3 μM for blebbistatin and azidoblebbistatin; the maximal extent of inhibition was 71% and 70%, respectively. (*Inset*) Irradiation of azidoblebbistatin before adding it to the protein completely abolished its inhibitory effect, whereas the same treatment did not affect blebbistatin inhibition. (*B*) Relative basal *DdMd* ATPase activities measured after a series of crosslinking rounds with azidoblebbistatin. Eight μM *DdMd* (M, column 1) was treated with 10 μM azidoblebbistatin (column 2), then crosslinked with UV light (column 3). The complex was further sequentially treated with 10-μM additions of azidoblebbistatin and UV irradiation (columns 4–10). In the reaction series, practically all myosin molecules were crosslinked, as indicated by the saturation in the inhibition of the ATPase activity. Importantly, ATPase activities were only affected by the covalently crosslinked azidoblebbistatin, because the azidoblebbistatin in solution was degradated completely. (*C*) Actin-activated ATPase activities of *DdMd* (in 50 μM actin) upon sequential azidoblebbistatin crosslinking cycles. Sequential 10 μM azidoblebbistatin addition plus UV irradiation cycles were performed on 4 μM DdMd. (*Inset*) The actin titration profile of untreated (□) and completely azidoblebbistatin-crosslinked (★) *DdMd*. Actin activated the untreated *DdMd* ATPase activity to a maximal extent of 1.4 ± 0.06 s^{-1} with half-maximal activation at 50 μM actin. In contrast, the ATPase activity of crosslinked *DdMd* remained unaffected by the presence of actin.

(Fig. 4). With respect to cell count, there was no significant difference between the cultures treated by the two inhibitors (Fig. 4*A*). Moreover, azidoblebbistatin administration combined with UV irradiation had a noticeably stronger inhibitory effect on cell growth than blebbistatin or azidoblebbistatin treatment

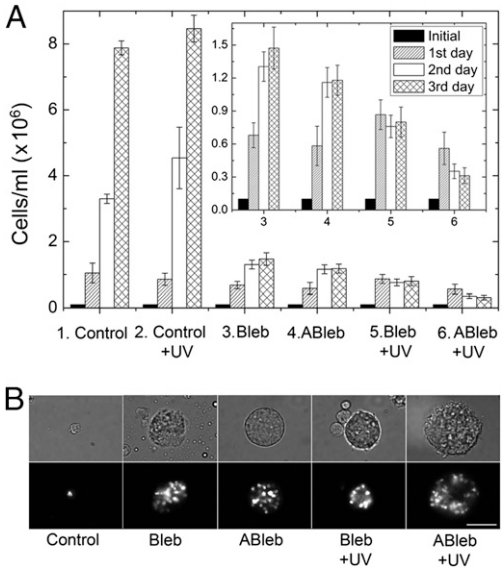

Fig. 4. Effect of azidoblebbistatin on *Dd* cells. (*A*) *Dd* ORF$^+$ cells were cultured for 3 d at 21 °C with shaking at 200 rpm. Next, 5 μM blebbistatin (Bleb), 5 μM azidoblebbistatin (ABleb) or an equivalent volume of DMSO (Control) was added to the cells each day for 3 d. UV irradiation was carried out in cell cultures each day for 5 min at 310 nm where indicated (+UV). Cell numbers were counted every 24 h. In the absence of irradiation, blebbistatin and azidoblebbistatin inhibited cell growth to a similar extent. Azidoblebbistatin treatment combined with UV irradiation proved to be most efficient in inhibiting cell growth. (*Inset*) Datasets 3–6 in a magnified scale. (*B*) After 3 d representative images were taken without and with nuclear staining (*Upper* and *Lower*, respectively). In the absence of irradiation, azidoblebbistatin and blebbistatin treatment resulted in practically identical *Dd* cell morphology. When inhibitor administration was combined with UV irradiation, azidoblebbistatin treatment resulted in a higher proportion of multinucleate cells with an increased average number of nuclei. (Scale bar, 50 μm.)

alone. It was shown by control experiments that UV irradiation at this wavelength did not inhibit cell growth in the absence of inhibitors (Fig. 4*A*).

Identification of High- and Low-Affinity Binding Partners of Azidoblebbistatin. To demonstrate the utility of azidoblebbistatin for the identification of proteins interacting with the inhibitor, we prepared *Dd* whole-cell lysates as well as myosin-enriched fractions of the lysates of a *Dd* cell line expressing recombinant *DdMd*, and subjected the samples to increasing concentrations of azidoblebbistatin and 310-nm irradiation. Samples were analyzed by SDS/PAGE alongside purified *DdMd* by using the fluorescence signal of azidoblebbistatin as well as by subsequent Coomassie staining (Fig. 5 *A* and *B*, and Fig. S2). We observed six distinct fluorescent bands in the myosin-enriched fractions, which were analyzed by densitometry and mass spectrometry (Fig. 5 *A*, *C–H* and Table 1). The analysis showed that azidoblebbistatin binds most specifically to myosin II heavy chain (EC_{50} = 5.1 ± 1.4 μM) and its degradation product (EC_{50} = 9.3 ± 3.7 μM) as well as *DdMd* (EC_{50} = 5.2 ± 0.8 μM).

Furthermore, previously unknown low-affinity ($EC_{50} \geq 50$ μM) interacting partners of azidoblebbistatin were also identified. These partners include vacuolar H^+-ATPase A subunit and RNA-binding region RNP-1 domain-containing protein (recovered from a single band, EC_{50} = 50 ± 31 μM), a protein termed "hypothetical protein DDB_G0275045" (National Center for Biotechnology Information-NR database) and malate dehydrogenase (recovered from a single band, EC_{50} = 55 ± 17 μM), and elongation factor 1α ($EC_{50} > 100$ μM).

Discussion

Here we report the synthesis and functional characterization of azidoblebbistatin, a photoinducible aryl azide derivative of blebbistatin. According to our results, in the absence of UV irradiation, blebbistatin and azidoblebbistatin exhibit identical myosin inhibition properties in vitro and in vivo (Figs. 3*A* and 4). Irradiation of the myosin-azidoblebbistatin complex at 310 nm efficiently induces a covalent crosslink between the enzyme and the inhibitor, leading to a stable inhibited state of myosin (Fig. 3 *B* and *C*). Importantly, a similar irradiation treatment of azidoblebbistatin in the absence of protein completely abolishes its inhibitory capability because of the photoinduced configurational rearrangement of the molecule.

Covalent crosslinking of myosin with the inhibitor eliminates practical limitations of the application of blebbistatin both in vitro and in vivo. In our experiments we found the water solubility of blebbistatin to be even lower (about 7 μM) (*SI Text*) than previously indicated (4), and its applicability is further impaired by its slow precipitation. Although the water solubility of azidoblebbistatin is identical to that of blebbistatin, the photoreaction with myosin allows practically complete crosslinking via sequential rounds of treatment at low azidoblebbistatin concentration combined with UV irradiation (Fig. 3 *B* and *C*).

The above properties of azidoblebbistatin indicate that it may become a useful tool in physiological and cell biological as well as structural investigations of the motor action of various myosin II isoforms. For example, the myosin II pool present in a cell or tissue at a given time point can be rapidly and irreversibly inactivated by azidoblebbistatin crosslinking, and the activity arising from subsequent protein synthesis can be separately followed. In addition, it has been shown that myosin II-independent processes in myosin II-null *Dd* cells, such as cell streaming and plaque expansion, are also inhibited by blebbistatin (12). These effects presumably result from molecular interactions of blebbistatin with partners other than myosin II. Our results also demonstrate that these interaction partners can be captured via azidoblebbistatin treatment followed by UV irradiation, and identified based on the fluorescence of azidoblebbistatin, which remains distinguishable even in covalently crosslinked adducts (Fig. 5). In this way, even weak-binding cellular interacting partners of azidoblebbistatin can be determined. This process confers a great advantage of the presented method over pull-down techniques. Our results also show that EC_{50} values of azidoblebbistatin crosslinking to myosin closely match those of the IC_{50} values of noncovalent inhibition (Figs. 3*A* and 5 *C–E*, and Table 1). Thus, azidation may prove a useful technology to determine the complete binding patterns and apparent binding strengths of inhibitors and drug molecules.

Azidoblebbistatin may also open new avenues in the investigation of the structural mechanism of myosin motor activity. For example, crosslinking of myosin with azidoblebbistatin in different nucleotide- and actin-bound states may stabilize important intermediates of force generation. Such a possibility is substantiated by our recent finding that the complex of myosin with ADP and blebbistatin adopts a previously inaccessible structural state resembling the start point of the powerstroke (13). In this as well as many other cases, the relatively low affinity of the ligands for the enzyme is the most severe technical hurdle in the way of detailed structural characterization, which can be overcome by covalent crosslinking to azidoblebbistatin.

Materials and Methods

Reagents. For reagents, (-)-Blebbistatin, *N*-iodosuccinimide, boron trifluoride dihydrate, sodium bisulfite, sodium bicarbonate, triethylamine, trifluoroacetic acid, sodium azide, copper(I) iodide, sodium ascorbate, N,N′-dimethylethylenediamine, acetonitrile, and methanol were purchased from Sigma-Aldrich.

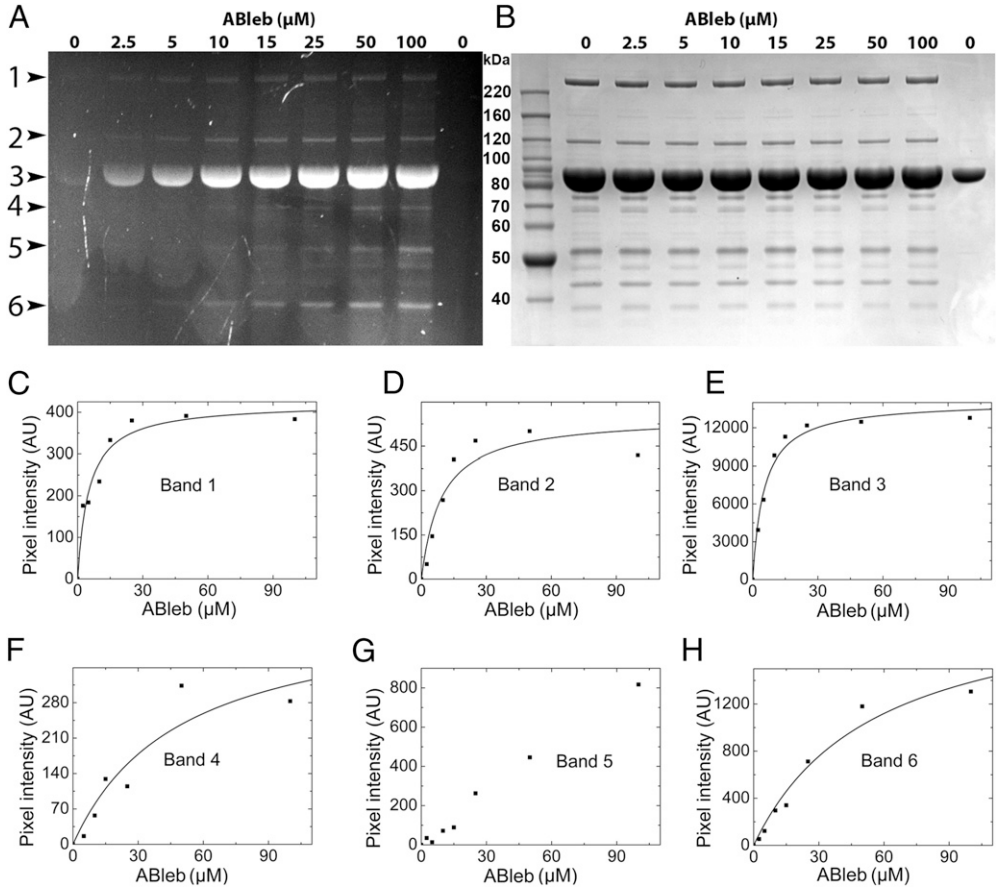

Fig. 5. SDS/PAGE analysis of azidoblebbistatin crosslinking of *Dd* proteins. Azidoblebbistatin-attached proteins in the myosin-enriched fraction of *DdMd*-expressing *Dd* cell lysates were detected by fluorescence of the covalently bound inhibitor (*A*) and, on the same gel, the protein contents were analyzed by subsequent Coomassie staining (*B*). Purified *DdMd* was loaded in the right-most lane of the gel as a control. Fluorescent bands are indicated at the left side of *A* in the order of increasing mobility. (*C*–*H*) Azidoblebbistatin concentration dependence of the fluorescence intensity of azidoblebbistatin-crosslinked protein bands. Hyperbolic fits to the datasets indicated high-affinity azidoblebbistatin binding in the case of bands in which the myosin II motor domain was present (*C*–*E*) and low-affinity binding in the case of other target proteins (*F* and *G*). Determined EC_{50} values are shown in Table 1.

Synthesis of Iodoblebbistatin. For iodoblebbistatin synthesis, 5 mg (-)-blebbistatin was dissolved in 300 μL methanol and transferred to a 10-mL microwave reaction vessel (CEM). During continuous stirring, 700 μL boron trifluoride dihydrate and 5.7 mg (1.5-fold excess) *N*-Iodosuccinimide was added and the reaction mixture was placed into a microwave reactor (CEM BenchMate 300W) at 50 °C for 30 min with magnetic stirring.

Purification of Iodoblebbistatin. A Strata XL 500 mg SPA column (Phenomenex) was equilibrated with 50 mL acetonitrile then 50 mL water and the crude reaction mixture was pipetted onto the column. It was sequentially washed with 20 mL water, 3 mL sodium bisulfite, 3 mL saturated sodium bicarbonate, 20 mL water, and then eluted with 20 mL acetonitrile containing 1% (vol/vol) trifluoroacetic acid and dried in vacuum. The brownish powder was dissolved in 0.5 mL acetonitrile containing 0.15% triethylamine (TEA) and it was further purified by HPLC (Agilent 1100 instrument) using a Luna 250 × 10 mm C18(2) column (Phenomenex). HPLC conditions were as follows: isocratic elution; content of buffer: water (0.15% TEA): acetonitrile (0.15% TEA) 3:7 (vol/vol); flow rate: 3.5 mL/min, detection wavelength: 254 nm.

Synthesis of Azidoblebbistatin. Pure iodoblebbistatin was dissolved in 1 mL of DMSO:H_2O mixture (5:1 vol/vol) and pipetted into a 10-mL reaction vessel containing 15 mg sodium azide, 2 mg copper(I) iodide, and 1 mg sodium ascorbate. Two micorliters N,N′-dimethylethylenediamine was added and the reaction mixture was stirred for 30 min at room temperature.

Purification of Azidoblebbistatin. The purification was performed in the same way as in case of iodoblebbistatin.

Table 1. Interacting partners of azidoblebbistatin identified by crosslinking, SDS/PAGE, and MS (Fig. 5 *B*–*D*)

Number of band	Identified protein	Molecular mass (kDa)	EC_{50} (μM)
1	Myosin II heavy chain	244	5.1 ± 1.4
2	Myosin II heavy chain degradation product	120	9.3 ± 3.7
3	Myosin motor domain	89	5.2 ± 0.8
4	Vacuolar H^+-ATPase A subunit and	69	50 ± 31
	RNA-binding region RNP-1 domain-containing protein	63	
5	Elongation factor 1α	50	>100
6	Hypothetical protein DDB_G0275045	37	55 ± 17
	Malate dehydrogenase	38	

Analytical HPLC. During the synthesis and in the further experiments analytical HPLC was performed using a Luna 250 × 4.6 mm C18(2) column (Phenomenex). HPLC conditions were identical to those described for the purification of iodoblebbistatin except that the flow rate was 1 mL/min.

Stock Solutions. For stock solutions, 100 mM azidoblebbistatin and 100 mM blebbistatin were prepared in DMSO and were used for further experiments.

Degradation Kinetics. For degradation kinetics, 0.5 mL 5 μM azidoblebbistatin solution in assay buffer (40 mM NaCl, 4 mM $MgCl_2$, 20 mM Hepes pH 7.3) was irradiated at 247, 278, and 310 nm (with 10-nm slit width) for 0 (control), 1, 2, and 5 min using an Edinburgh Instruments F900 Fluorescence Spectrometer equipped with a 450 W Xenon Lamp. At each time point, 10 μL solution was taken and analyzed by HPLC using conditions described above.

Basal ATPase Measurements. Relative basal ATPase activities of 2 μM or 8 μM *DdMd* W501+ construct (27) were measured at increasing concentrations of blebbistatin or azidoblebbistatin using a pyruvate kinase/lactate dehydrogenase coupled assay (NADH-coupled assay) (28) following absorbance at 340 nm. Measurements were carried out at 20 °C in an assay buffer described in *Degradation Kinetics*, without reducing agents that could interfere with the azide group. UV treatment was carried out at 310 nm for 3 min in the same way as described in *Degradation Kinetics*.

Actin-Activated ATPase Measurements. Four μM *DdMd* was crosslinked via sequential rounds of 10 μM azidoblebbistatin addition and UV irradiation. Following each crosslinking cycle, the ATPase activity of myosin was measured before and after the addition of 50 μM actin. The ATPase activity of completely crosslinked *DdMd* was also measured at increasing actin concentrations (0–80 μM) by the NADH-coupled assay described above. Actin was purified and prepared as described previously (29). A 1.5-fold molar excess of phalloidin (Sigma) was used to stabilize actin filaments.

Cell Culture Experiments. *Dd* ORF$^+$ cells were cultured in 50-mL Falcon tubes for 3 d at 21 °C with shaking at 200 rpm. Each day, 5 μM blebbistatin, 5 μM azidoblebbistatin, or equivalent volume of DMSO (control) were administered to the cells, and half of the cultures were also treated with 313-nm UV irradiation using an optical fiber-equipped mercury-xenon lamp (BioLogic Science Instruments; 200 W). Cell numbers were counted each day. After 3 d, cells were stained with Hoechst to visualize nuclei and imaged.

Preparation of *Dd* Whole-Cell Lysates and Myosin-Enriched Fractions. *Dd* ORF$^+$ cells were cultured, collected, and lysed as previously described (27). Whole-cell lysates were centrifuged at 12,100 × *g* for 30 min at 4 °C in a tabletop centrifuge, and supernatants were used for analysis. Myosin-enriched fractions were prepared by ultracentrifugation of the lysates for 60 min at 340,000 × *g* in a Beckman 55.1 Ti rotor in the absence of ATP, washing the pellet in a similar ultracentrifugation step, and subsequent release of ATP-sensitive proteins by ultracentrifugation in the presence of 20 mM MgATP. Supernatants of the last step were analyzed as "myosin-enriched fraction." This fraction is dominantly a crude sample of actin and microtubule binding proteins which can be dissociated by ATP.

Azidoblebbistatin Crosslinking and Analysis of *Dd* Cell Lysates and Myosin-Enriched Fractions. Whole-cell lysates and myosin-enriched fractions were crosslinked with azidoblebbistatin at concentrations of 2.5, 5, 10, 15, 25, 50, and 100 μM. Samples were irradiated in one round for 10 min after azidoblebbistatin addition. The optical arrangement was as described in *Degradation Kinetics*. The protein content of the samples was analyzed by SDS/PAGE using UV transillumination to detect azidoblebbistatin fluorescence, and also by subsequent Coomassie staining using a Syngene Gene Genius Bio Imaging System.

Mass Spectrometry of Protein Bands. Fluorescent SDS/PAGE bands gel were excised, alkylated with iodoacetamide and digested with trypsin for 4 h at 37 °C. After extraction, samples were dried and resolved in 10 μl of 1% formic acid. Mass spectrometry was carried out using a Waters Q-TOF instrument. Data were analyzed using the Mascot Distiller program.

ACKNOWLEDGMENTS. This work was funded by the Hungarian Academy of Sciences, HAS-ELTE research group ID: 01055 (to A.M.-C); Norway Grant NNF2-85613 (to M. Kovács); Hungarian Scientific Research Fund K71915 (to M. Kovács); the "Momentum" Program of the Hungarian Academy of Sciences LP2011-006/2011 (to M. Kovács); the European Research Council (European Community's Seventh Framework Programme FP7/2007-2013)/European Research Council Grant Agreement 208319 (to A.M.-C); the National Development Agency under the aegis of the National Technology Programme (NTP TECH_08_A1/2-2008-0106) (to A.M.-C.); and the European Union cofinanced by the European Social Fund (TAMOP 4.2.1/B-09/1/KMR-2010-0003) (to M. Kovács and A.M.-C.). M. Kovács and A.B. are Bolyai Fellows of the Hungarian Academy of Sciences.

1. Herrmann C, Wray J, Travers F, Barman T (1992) Effect of 2,3-butanedione monoxime on myosin and myofibrillar ATPases. An example of an uncompetitive inhibitor. *Biochemistry* 31:12227–12232.
2. Higuchi H, Takemori S (1989) Butanedione monoxime suppresses contraction and ATPase activity of rabbit skeletal muscle. *J Biochem* 105:638–643.
3. Cheung A, et al. (2002) A small-molecule inhibitor of skeletal muscle myosin II. *Nat Cell Biol* 4:83–88.
4. Straight AF, et al. (2003) Dissecting temporal and spatial control of cytokinesis with a myosin II Inhibitor. *Science* 299:1743–1747.
5. Kovács M, Tóth J, Hetényi C, Málnási-Csizmadia A, Sellers JR (2004) Mechanism of blebbistatin inhibition of myosin II. *J Biol Chem* 279:35557–35563.
6. Ramamurthy B, Yengo CM, Straight AF, Mitchison TJ, Sweeney HL (2004) Kinetic mechanism of blebbistatin inhibition of nonmuscle myosin IIb. *Biochemistry* 43: 14832–14839.
7. Ostap EM (2002) 2,3-Butanedione monoxime (BDM) as a myosin inhibitor. *J Muscle Res Cell Motil* 23:305–308.
8. Chinthalapudi K, et al. (2011) Mechanism and specificity of pentachloropseudilin-mediated inhibition of myosin motor activity. *J Biol Chem* 286:29700–29708.
9. Martin R, et al. (2009) Total synthesis of pentabromo- and pentachloropseudilin, and synthetic analogues—Allosteric inhibitors of myosin ATPase. *Angew Chem Int Ed Engl* 48:8042–8046.
10. Preller M, Chinthalapudi K, Martin R, Knolker HJ, Manstein DJ (2011) Inhibition of Myosin ATPase activity by halogenated pseudilins: A structure-activity study. *J Med Chem* 54:3675–3685.
11. Limouze J, Straight AF, Mitchison T, Sellers JR (2004) Specificity of blebbistatin, an inhibitor of myosin II. *J Muscle Res Cell Motil* 25:337–341.
12. Shu S, Liu X, Korn ED (2005) Blebbistatin and blebbistatin-inactivated myosin II inhibit myosin II-independent processes in *Dictyostelium*. *Proc Natl Acad Sci USA* 102: 1472–1477.
13. Takács B, et al. (2010) Myosin complexed with ADP and blebbistatin reversibly adopts a conformation resembling the start point of the working stroke. *Proc Natl Acad Sci USA* 107:6799–6804.
14. Vodovozova EL (2007) Photoaffinity labeling and its application in structural biology. *Biochemistry (Mosc)* 72:1–20.
15. Filer CN (2009) Tritium labelled photoaffinity agents. *J Radioanal Nucl Chem* 281: 521–530.
16. Evans RK, Haley BE (1987) Synthesis and biological properties of 5-azido-2′-deoxyuridine 5′-triphosphate, a photoactive nucleotide suitable for making light-sensitive DNA. *Biochemistry* 26:269–276.
17. Andersen J, et al. (2005) Rapid synthesis of aryl azides from aryl halides under mild conditions. *Synlett* (14):2209–2213.
18. Castanet AS, Colobert F, Broutin PE (2002) Mild and regioselective iodination of electron-rich aromatics with *N*-iodosuccinimide and catalytic trifluoroacetic acid. *Tetrahedron Lett* 43:5047–5048.
19. Hegyi G, Szilagyi L, Elzinga M (1986) Photoaffinity labeling of the nucleotide binding site of actin. *Biochemistry* 25:5793–5798.
20. Prakash GKS, et al. (2004) N-halosuccinimide/BF3-H2O, efficient electrophilic halogenating systems for aromatics. *J Am Chem Soc* 126:15770–15776.
21. Scheurich P, Schäfer HJ, Dose K (1978) 8-Azido-adenosine 5′-triphosphate as a photoaffinity label for bacterial F1 ATPase. *Eur J Biochem* 88:253–257.
22. Mo F, et al. (2010) Gold-catalyzed halogenation of aromatics by N-halosuccinimides. *Angew Chem Int Ed Engl* 49:2028–2032.
23. Lucas-Lopez C, et al. (2005) Absolute stereochemical assignment and fluorescence tuning of the small molecule tool, (-)-blebbistatin. *Eur J Org Chem* (9):1736–1740.
24. Volman DH, Hammond GS, Neckers DC, eds (1992) *Advances in Photochemistry* (Wiley-Interscience, New York), Vol 17, pp 69–143.
25. Kolega J (2004) Phototoxicity and photoinactivation of blebbistatin in UV and visible light. *Biochem Biophys Res Commun* 320:1020–1025.
26. Sakamoto T, Limouze J, Combs CA, Straight AF, Sellers JR (2005) Blebbistatin, a myosin II inhibitor, is photoinactivated by blue light. *Biochemistry* 44:584–588.
27. Málnási-Csizmadia A, Woolley RJ, Bagshaw CR (2000) Resolution of conformational states of *Dictyostelium* myosin II motor domain using tryptophan (W501) mutants: Implications for the open-closed transition identified by crystallography. *Biochemistry* 39:16135–16146.
28. Gyimesi M, et al. (2008) The mechanism of the reverse recovery step, phosphate release, and actin activation of *Dictyostelium* myosin II. *J Biol Chem* 283:8153–8163.
29. Pardee JD, Spudich JA (1982) Purification of muscle actin. *Methods Cell Biol* 24: 271–289.